International Journal of

HEAT and MASS TRANSFER

Available online at www.sciencedirect.com

SciVerse ScienceDirect

Specific absorption rate and temperature increase in the human eye due to electromagnetic fields exposure at different frequencies

Teerapot Wessapan [a], Phadungsak Rattanadecho [b,*]

[a] School of Aviation, Eastern Asia University, Pathumthani 12110, Thailand
[b] Center of Excellence in Electromagnetic Energy Utilization in Engineering (CEEE), Department of Mechanical Engineering, Faculty of Engineering, Thammasat University (Rangsit Campus), Pathumthani 12120, Thailand

ARTICLE INFO

ABSTRACT

This study presents a numerical analysis of the specific absorption rate (SAR) and the heat transfer in a heterogeneous human eye model exposed to electromagnetic (EM) fields of 900 and 1800 MHz. In this study, the effect of operating frequency on the SAR and temperature distributions in the eye was systematically investigated. The SAR value and the temperature distribution in various tissues in the eye during exposure to EM fields were obtained by numerical simulation of EM wave propagation and a heat transfer model was then developed based on the natural convection and porous media theories. The study highlights two transport phenomena: heat and mass transfer in the eye during exposure to EM fields at different frequencies. This study indicated that when the eye exposed to EM fields at the frequencies of 900 and 1800 MHz, the highest SAR values at two chosen frequencies was in the cornea, and the highest temperature at the frequency of 900 MHz was in the anterior chamber while the highest for the frequency of 1800 MHz was in the vitreous. The temperature distribution in the eye induced by EM fields was not directly related to the SAR distribution due to the effect of the interaction among the dielectric properties, thermal properties, blood perfusion, and penetration depth of the EM power. Moreover, this study also showed that the exposure time had an influence on the temperature increase in the eye.

1. Introduction

The electromagnetic (EM) waves of different power levels and frequencies penetrate deep into the human body causing health risks. In recent years, there has been increasing public concern with the interaction between the human body and the EM fields. Since the human eye is one of the most sensitive organs to the EM radiation. The high intensity EM fields can lead to a number of ocular effects. However, the resulting thermo-physiologic response of the eye to EM fields is still not well understood. In order to gain insight into the phenomena of heat and mass transfer in the eye concerned with the temperature distribution induced by EM fields, a detailed knowledge of the absorbed power distribution as well as the temperature distribution are necessary. Therefore, this study investigates the ocular effects occurred during exposure to EM fields. Although the safety standards in term of the maximum SAR values are regulated, but they are not stated in term of the maximum temperature increase in the eye caused by EM energy absorption which is an actual influence of the dominant factors inducing the adverse physiological effects. The severity of

these effects produced by increasing a small temperature can cause eyesight to worsen. There have been medical case reports of the formation of cataracts in humans following accidental exposure to microwave radiation [1]. Actually, a small temperature increase of 3–5 °C in the eye leads to induce cataracts formation [2]. Additionally, it is reported that the temperature above 41 °C is necessary for production of posterior lens opacities [3]. Numerical analysis of the heat and mass transfer in the eye exposed to EM fields has provided useful information on absorption of EM energy for the eye under a variety of exposure conditions.

In the past, there have been reports on the effects of EM fields on the eye [4,5]. Nevertheless, the analysis generally was conducted based on the maximum SAR values permitted by public safety standards [6,7]. The experimental data on the correlation between the SAR levels and the temperature increase in the human tissue was still sparse. Most previous studies of human exposed to EM fields hardly considered the heat transfer causing an incomplete analysis to the results. Therefore, modeling of heat transport in human tissue is needed to cooperate with the modeling of EM in order to completely explain their interaction characteristics for approaching such phenomena.

The topic of temperature increase in human tissue when exposed to EM fields, particularly those radiated to the eye, has been of inter-

Nomenclatures

C	specific heat capacity (J/(kg K))
E	electric field intensity (V/m)
e	tear evaporation heat loss (W/m^2)
f	frequency of incident wave (Hz)
H	magnetic field (A/m)
h	convection coefficient (W/m^2 K)
j	current density (A/m^2)
k	thermal conductivity (W/(m K))
n	normal vector
p	pressure (N/m^2)
Q	heat source (W/m^3)
T	temperature (K)
u	velocity (m/s)
t	time

Greek letters

B	volume expansion coefficient (1/K)
μ	magnetic permeability (H/m)

ε	permittivity (F/m)
σ	electric conductivity (S/m)
ω	angular frequency (rad/s)
ρ	density (kg/m^3)
ω_b	blood perfusion rate (1/s)
Γ	external surface area

Subscripts

am	ambient
b	blood
ext	external
i	subdomain
met	metabolic
r	relative
ref	reference
0	free space, initial condition

est for many years. Recently, the modeling of heat transport in human tissue has been investigated by many researchers [8–21]. The thermal modeling of human tissue is important as a tool to investigate the effect of external heat sources and to predict the abnormalities in the tissue. In the past, most studies of heat transfer analysis in the eye used heat conduction equation [8–14]. Some studies carried out on the natural convection in the eye based on heat conduction model [15,16]. Ooi and Ng [16,17] studied the effect of aqueous humor (AH) hydrodynamics on the heat transfer in the eye based on heat conduction model. Meanwhile, the bioheat equation, introduced by Pennes [18,19] based on the heat diffusion equation for a blood perfused tissue, is used for modeling of the heat transfer in the eye as well [20,21]. Ooi and Ng also developed a three-dimensional model of the eye [22], extending their two-dimensional model [21]. Recently, porous media models have been utilized to investigate the transport phenomena in biological media instead of a simplified bioheat model [23–25]. Shafahi and Vafai [26] proposed the porous media along with a natural convection model to analyze the eye thermal characteristics during exposure to thermal disturbances. The other research groups have been tried to conduct the advanced model using a coupled model of heat and EM dissipation in the eye [10–14]. Ooi et al. have been tried to conduct the advanced model using the coupled model of heat and laser irradiation in the eye [27]. Results from a similar model of Ooi et al. [27] for various applications were also presented in continuation [28–31].

Our research group has tried to numerically investigate the temperature increase in the human tissue subjected to EM fields in many problems [32–38]. Wessapan et al. [32,33] utilized a 2D finite element method to obtain the SAR and temperature increase in the human body exposed to leakage EM waves. Wessapan et al. [34,35] developed a three-dimensional human head model in order to investigate the SAR and temperature distributions in human head during exposure to the mobile phone radiation. Keangin et al. [36,37] carried out on the numerical simulation of the liver cancer treated using the complete mathematical model considered the coupled model of EM wave propagation, heat transfer and mechanical deformation in the biological tissue in the couple's way. Wessapan et al. [38] investigated the SAR and temperature distributions in the eye during exposed to EM waves at 900 MHz using the porous media theory.

Most previous studies of the interaction between the EM fields and the eye mainly focused on SAR. They have not been considered

heat transfer causing an incomplete analysis of results. Therefore, the modeling of the heat transport is needed to completely explain the actual process of interaction between the EM fields and the eye. Although the porous media and natural convection models of the eye have been used in the previous biomedical studies [15,16,26], most studies of the human eye exposed to the EM fields, especially at different frequencies, have not been considering the porous media and natural convection approaches is sparse or non-existent.

There are few studies on the temperature and EM field interaction in a realistic physical model of the human organs especially the eye due to the complexity of the problem, even though it is directly related to the thermal injury of tissues. Therefore, in order to provide information on the levels of exposure and health effects from the different frequencies of EM field exposure adequately, it is essential to simulate both of the EM fields and the heat transfer based on the porous media theory in an anatomical model particularly the eye.

This study presents the simulation of the SAR and temperature distributions in an anatomical human eye exposed to EM fields based on the porous media theory. The work described in this paper is substantially extended from our previous work [38] by further enhancing the focus on the effect of operating frequency. In this study, a two-dimensional human eye model was used to simulate the SAR and temperature distributions in the eye model. The EM wave propagation in the eye was investigated by using Maxwell's equations. An analysis of the heat transfer in the eye exposed to TM-mode of EM fields at different frequencies was investigated using a developed heat transfer model (included the conduction and natural convection heat transfer modes) which was firstly proposed by Shafahi and Vafai [26]. In the heterogeneous eye model, the effect of operating frequency on the SAR and temperature distributions in the eye is systematically investigated. The SAR and temperature distributions are studied in various parts of the eye during exposure to EM fields of 900 and 1800 MHz. They are obtained by numerical simulation of the EM wave propagation and heat transfer equations, are presented. In this study, the frequencies of 900 and 1800 MHz were chosen for our simulations and the frequencies used globally in a wide range of applications including Global System for Mobile Communications (GSM) services. In this work, the model excluded the presence of eyelid as well as the metabolic heat generation in order to ease the modeling procedures. The obtained

values represent the accurate phenomena to determine the temperature increase in the eye and indicate the limitations that must be considered as the temperature increase due to EM energy absorption from EM field exposure at different frequencies.

2. Formulation of the problem

Fig. 1 shows the radiation of the EM fields from an EM radiation device to the eye. These EM fields fall on the eye that causes heating in the deeper tissue, which leads to tissue damage and cataract formation. Due to ethical consideration, exposing the human to EM fields for experimental purposes is limited. It is more convenient to develop a realistic human eye model through the numerical simulation. A highlight of this work is the illustration of the transport phenomena, including the heat and mass transfer in the eye during exposure to EM fields at different frequencies. The analyses of the SAR and the heat transfer in the eye exposed to EM fields will be illustrated in Section 3. The system of governing equations as well as the initial and boundary conditions are solved numerically using the finite element method (FEM) via COMSOL™ Multiphysics.

3. Methods and model

The first step in evaluating the effects of a certain exposure to EM fields in the eye is to determine the induced internal EM fields and its spatial distribution. Thereafter, EM energy absorption which results in temperature increase in the eye and other interactions will be able to be considered.

3.1. Physical model

In this study, the two-dimensional model of the eye, which follows the physical model in the previous research [26], is developed. Fig. 2 shows the two-dimensional eye model used in this study. This model comprises seven types of tissue including cornea, anterior chamber, posterior chamber, iris, sclera, lens and vitreous. These tissues have the different dielectric and thermal properties. In the sclera layer, there are two more layers known as the choroid and retina which are relatively thin compared to the sclera. To simplify the problem, these layers are assumed to be homogeneous. The iris and sclera, which have the same properties, are modeled together as one homogenous region [16]. The dielectric and thermal properties of tissue are given in Tables 1 and 2, respectively. Each tissue is assumed to be homogeneous and electrically as well as thermally isotropic.
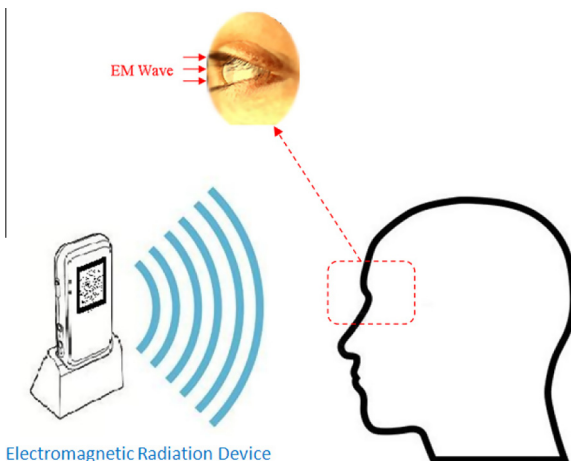

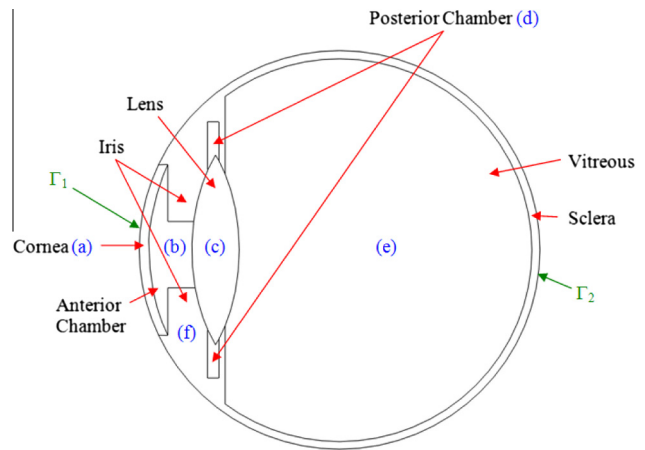**Fig. 1.** EM fields from an EM radiation device.

Fig. 2. Human eye vertical cross section.

Table 1
Dielectric properties of tissues at 900 MHz and 1800 MHz [39,40,23].

Tissue	Frequency: 900 MHz		Frequency: 1800 MHz	
	ε_r	σ (S/m)	ε_r	σ (S/m)
Cornea (a)	52.0	1.85	55.0	2.32
Anterior chamber (b)	73.0	1.97	75.0	2.40
Lens (c)	51.3	0.89	41.1	1.29
Posterior chamber (d)	73.0	1.97	75.0	2.40
Vitreous (e)	74.3	1.97	73.7	2.33
Sclera (f)	52.1	1.22	52.7	1.68
Iris (f)	52.1	1.22	52.7	1.68

3.2. Equations for EM wave propagation analysis

The mathematical models are developed to predict the electric fields and the SAR with respect to the temperature gradient in the eye. To simplify the problem, the following assumptions are made:

1. The EM wave propagation is modeled in two dimensions.
2. The eye in which the EM waves interact with the eye proceeds in the open region.
3. The free space is truncated by scattering boundary condition.
4. The model assumes that dielectric properties of each tissue are constant.
5. In the eye, the EM waves are characterized by transverse magnetic fields (TM-mode).

The EM wave propagation in the eye is calculated using Maxwell's equations which mathematically describe the interdependence of the EM waves. The general form of Maxwell's equations is simplified to demonstrate the EM fields penetrated in the eye as the following equation:

$$\nabla \times \left(\left(\varepsilon_r - \frac{j\sigma}{\omega\varepsilon_0} \right)^{-1} \nabla \times H_z \right) - \mu_r k_0^2 H_z = 0 \tag{1}$$

where H is the magnetic field (A/m), μ_r is the relative magnetic permeability, ε_r is the relative dielectric constant, $\varepsilon_0 = 8.8542 \times 10^{-12}$ F/m is the permittivity of free space, k_0 is the free space wave number (m^{-1}).

3.2.1. Boundary condition for wave propagation analysis

EM energy is emitted by an EM radiation device and falls on the eye with a particular power density. Therefore, boundary condition for solving EM wave propagation, as shown in Fig. 3, is described as follows:

Table 2
Thermal properties of the eye [16].

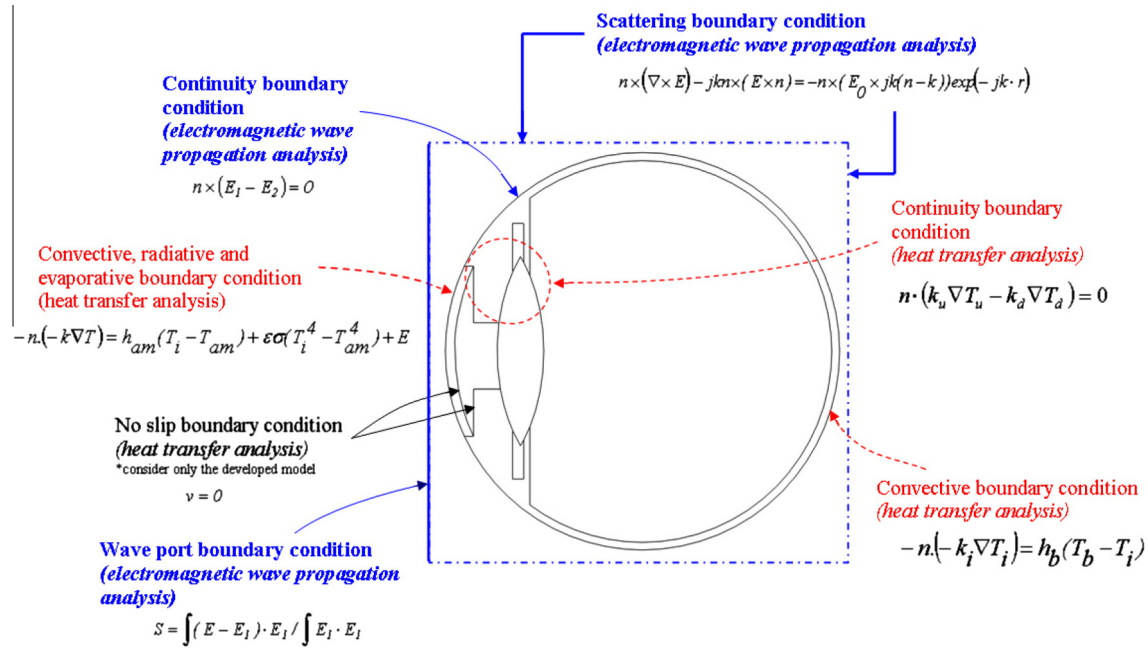| Tissue	ρ (kg/m³)	k (W/m C)	C_p (J/kg C)	μ (N s/m²)	β (1/K)
Cornea (a)	1050	0.58	4178	–	–
Anterior chamber (b)	996	0.58	3997	0.00074	0.000337
Lens (c)	1000	0.4	3000	–	–
Posterior chamber (d)	996	0.58	3997	–	–
Vitreous (e)	1100	0.603	4178	–	–
Sclera (f)	1050	1.0042	3180	–	–
Iris (f)	1050	1.0042	3180	–	–

Fig. 3. Boundary condition for analysis of EM wave propagation and heat transfer.

It is assumed that the uniform wave flux falls on the left side of the eye. Therefore, at the left boundary of the considered domain, an EM simulator employs TM wave propagation port with specified power density,

$$S = \int (E - E_1) \cdot E_1 \Big/ \int E_1 \cdot E_1 \tag{2}$$

Boundary conditions along the interfaces between different mediums, for example, between air and tissue or tissue and tissue, are considered as continuity boundary condition,

$$n \times (E_1 - E_2) = 0 \tag{3}$$

The outer sides of the calculated domain, i.e., free space, are considered as scattering boundary condition [25],

$$n \times (\nabla \times E_z) - jkE_z = -jk(1 - k \cdot n)E_{0z}\exp(-jk \cdot r) \tag{4}$$

where k is the wave number (m^{-1}), σ is the electrical conductivity (S/m), n is the normal vector, $j = \sqrt{-1}$, and E_0 is the incident plane wave (V/m).

3.3. Interaction of EM fields and human tissues

Interaction of EM fields with biological tissue can be defined in the term of the SAR. When the EM waves propagate through the tissue, the energy of EM waves is absorbed by the tissue. The SAR is defined as power dissipation rate normalized by material density [25]. The SAR is given by,

$$SAR = \frac{\sigma}{\rho}|E|^2 \tag{5}$$

where E is the electric field intensity (V/m), σ is the electric conductivity (S/m), and ρ is the tissue density (kg/m³).

3.4. Equations for heat transfer and flow analysis

To solve the thermal problem, the coupled effects of the EM wave propagation and the unsteady bioheat transfer are investigated. The temperature distribution is corresponded to the SAR. This is because the SAR in the eye distributes owing to energy absorption. Thereafter, the absorbed energy is converted to thermal energy, which increases the tissue temperature. Heat transfer analysis of the eye is modeled in two dimensions. To simplify the problem, the following assumptions are made:

1. The Human tissue is a bio-material with constant thermal properties.
2. There is no phase change of substance in the tissue.
3. There is a local thermal equilibrium between the blood and the tissue.
4. There is no chemical reaction in the tissue.

This study utilized the pertinent thermal model based on the porous media theory [26] to investigate the heat transfer behavior of the eye when exposed to the EM fields.

In this study, the motion of fluid is considered only inside the anterior chamber [16]. There is a blood flow in the iris/sclera part, which plays a role to adjust the eye temperature with the rest of the body [26]. For the rest parts, the metabolic heat generation is neglected based on the fact that these comprise mainly water [16]. The equation governing the flow of heat in cornea, posterior chamber, lens and vitreous are resembled the classical heat conduction equation given in Eq. (6)

$$\rho_i C_i \frac{\partial T_i}{\partial t} = \nabla \cdot (k_i \nabla T_i) + Q_{ext}; \quad i = a, c, d, e \tag{6}$$

This model accounts for the existence of AH in the anterior chamber. The heat transfer process consists of both the conduction and natural convections, which can be written as follows:

Continuity equation:

$$\nabla \cdot u_i = 0; \quad i = b \tag{7}$$

Momentum equation:

$$\rho_i \frac{\partial u_i}{\partial t} + \rho_i u_i \nabla \cdot u_i = -\nabla p_i + \nabla \cdot [\mu(\nabla u_i + \nabla u_i^T)]$$
$$+ \rho_i g \beta_i (T_i - T_{ref}); \quad i = b \tag{8}$$

where i denotes each subdomain in the eye model as shown in Fig. 2, ρ is the tissue density (kg/m³), β is the volume expansion coefficient (1/K), u is the velocity (m/s), p is the pressure (N/m²), μ is the dynamic viscosity of AH (N s/m²), t is the time, T is the tissue temperature (K), and T_{ref} is the reference temperature considered here is 37 °C. The effects of buoyancy due to the temperature gradient are modeled using the Boussinesq approximation which states that the density of a given fluid changes slightly with temperature but negligibly with pressure [16].

Energy equation:

$$\rho_i C_i \frac{\partial T_i}{\partial t} - \nabla \cdot (k_i \nabla T_i) = -\rho C_i u_i \cdot \nabla T_i + Q_{ext}; \quad i = b \tag{9}$$

The sclera/iris is modeled as a porous medium with the blood perfusion, which assumes that local thermal equilibrium exits between the blood and the tissue. The blood perfusion rate used is 0.004 1/s. A modified Pennes' bioheat equation [26,23] is used to calculate the temperature distribution in the sclera/iris

$$(1 - \varepsilon)\rho_i C_i \frac{\partial T_i}{\partial t} = \nabla \cdot ((1 - \varepsilon)k_i \nabla T_i) + \rho_b C_b \omega_b (T_b - T_i) + Q_{ext}; \quad i = f \tag{10}$$

where C is the heat capacity of tissue (J/kg K), k is the thermal conductivity of tissue (W/m K), T_b is the temperature of blood (K), ρ_b is the density of blood (kg/m³), C_b is the specific heat capacity of blood (J/kg K), ω_b is the blood perfusion rate (1/s), and Q_{ext} is the external heat source term (EM heat-source density) (W/m³).

In the analysis, the porosity (ε) used is assumed to be 0.6. The heat conduction between the tissue and the blood flow is approximated by the blood perfusion term, $\rho_b C_b \omega_b (T_b - T)$.

The external heat source term is equal to the resistive heat generated by the EM fields (EM power absorbed), which defined as [32]

$$Q_{ext} = \frac{1}{2} \sigma_{tissue} |\bar{E}|^2 = \frac{\rho}{2} \cdot \text{SAR} \tag{11}$$

where σ_{tissue} is the electric conductivity of tissue (S/m).

3.4.1. Boundary condition for heat transfer analysis

The heat transfer analysis excluding the surrounding space is considered only in the eye. The cornea surface as shown in Fig. 3, is considered as the convective, radiative, and evaporative boundary conditions.

$$-n(-k\nabla T) = h_{am}(T_i - T_{am}) + \varepsilon\sigma(T_i^4 - T_{am}^4) + e \quad \text{on } \Gamma_1 \quad i = \alpha \tag{12}$$

where Γ_i is the external surface area corresponding to section i, e is the tear evaporation heat loss (W/m²), T_{am} is the ambient temperature (K), h_{am} is the convection coefficient (W/m² K).

The temperature of blood generally assumed to be the same as the body core temperature causes heat to be transferred into the eye [16]. The surface of the sclera is assumed to be a convective boundary condition

$$-n \cdot (-k_i \nabla T_i) = h_b(T_b - T_i) \quad \text{on } \Gamma_2 \quad i = f \tag{13}$$

where h_b is the convection coefficient of blood (65 W/m² K). Γ_1 and Γ_2 are the corneal surface and sclera surface of the eye, respectively.

3.5. Calculation procedure

In this study, the finite element method is used to analyze the transient problems. The computational scheme is to assemble finite element model and compute a local heat generation term by performing an EM calculation using tissue properties. In order to obtain a good approximation, a fine mesh is specified in the sensitive areas. This study provides a variable mesh method for solving the problem as shown in Fig. 4. The system of governing equations as well as the initial and boundary conditions are then solved. All computational processes are implemented using COMSOL™ Multi-
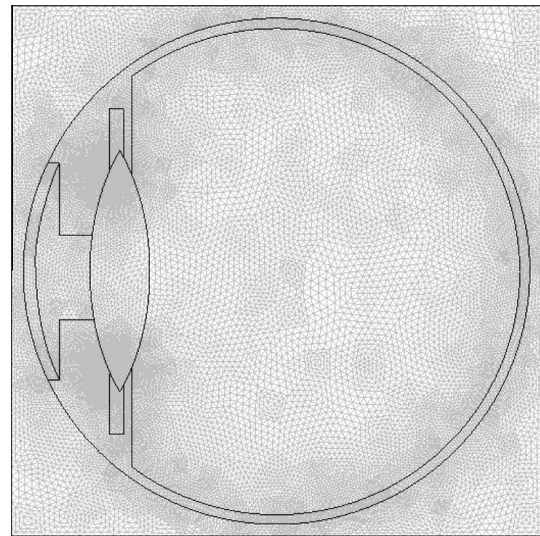
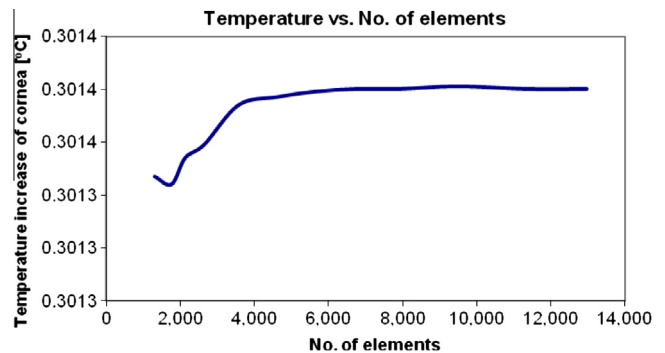**Fig. 4.** A two-dimensional finite element mesh of human eye model.

Fig. 5. Grid convergence curve of the 2D model.

physics, to demonstrate the phenomenon that occurs in the eye exposed to the EM fields.

The 2D model is discretized using triangular elements and the Lagrange quadratic is then used to approximate the temperature and SAR variations across each element. The convergence test is carried out to identify the suitable number of elements required. The convergence curve resulting from the convergence test is shown in Fig. 5. This convergence test leads to the grid with approximately 10,000 elements. It is reasonable to assume that, at this element number, the accuracy of the simulation results is independent from the number of elements.

4. Results and discussion

In this study, the coupled model of the EM and thermal fields are solved numerically. For the simulation, the dielectric and thermal properties are directly taken from Tables 1 and 2, respectively. The exposed radiated power used in this study refers to the International Commission of Non-Ionizing Radiation Protection (IC-NIRP) standard for safety level at the maximum SAR value of 2 W/kg (general public exposure) and 10 W/kg (occupational exposure) [6]. Since most GSM networks use frequencies in the 900 and 1800 MHz spectrum, therefore, in this analysis, the effects of these operating frequencies on distributions of SAR and temperature in the eye are systematically investigated.

4.1. Verification of the model

In order to verify the accuracy of the present numerical models, the case without EM fields of the simulated results from this study are validated against the numerical results with the same geometric model obtained by Shafahi and Vafai [26]. Moreover, the numerical results are then compared to the experimental results of the rabbit obtained from Lagendijk [8]. The validation case assumes that the rabbit body temperature is 38.8 °C, the tear evaporation heat loss is 40 W/m², the ambient temperature is 25 °C, and the convection coefficient of ambient air is 20 W/m² K. The results of the selected test case are depicted in Fig. 6 for temperature distribution in the eye. Fig. 6 clearly shows a good agreement of the

temperature distribution in the eye between the present solution and that of Shafahi and Vafai [26] and Lagendijk [8]. In the figure, the simulated results provides a good agreement with the simulated results obtained from Shafahi and Vafai [26]. This favorable comparison lends confidence in the accuracy of the present numerical model.

4.2. Electric field distribution

In order to study the effect of operating frequency, the eye is exposed to the power density of 100 mW/cm² at the frequencies of 900 and 1800 MHz. To illustrate the penetrated electric field distribution inside the eye, the predicted results obtained from our proposed models are required. Fig. 7 shows the simulation of an electric field pattern inside the eye exposed to the EM fields in TM mode operating at the frequencies of 900 and 1800 MHz propagating along the vertical cross section human eye model. Due to the different dielectric characteristics of the various tissue layers at different operating frequencies, a different fraction of the supplied EM energy will become absorbed in each layer in the eye. Consequently, the reflection and transmission components at each layer contribute to the resonance of standing wave in the eye. It can be seen that the higher values of electric fields at the both frequencies occur in the outer part area of the eye, especially in cornea, and lens. By comparison, the maximum electric field intensity in outer parts of the eye at the frequency of 900 MHz displays a higher value than that of 1800 MHz. The maximum electric field intensities are 391.8 and 231.2 V/m at the frequencies of 900 and 1800 MHz, respectively. The maximum value for the frequency of 900 MHz is in the cornea while for the frequency of 1800 MHz is in the lens. Mathematically, this result corresponds to Eq. (1) and the dielectric properties (ε_r) in Table 1 show that the frequency of 900 MHz has lower dielectric properties of cornea, while the frequency of 1800 MHz has lower dielectric properties of lens. It is found that these alterations of electric field distribution between the two chosen frequencies vary in extent with the magnitude of the dielectric property and with the standing-wave pattern. For both frequencies, the electric fields deep inside the eye are extinguished where the electric fields attenuate due to the absorbed EM energy and are then converted to heat. Moreover, the electric field distribution also showed a strong dependence on the dielectric properties of the tissue.
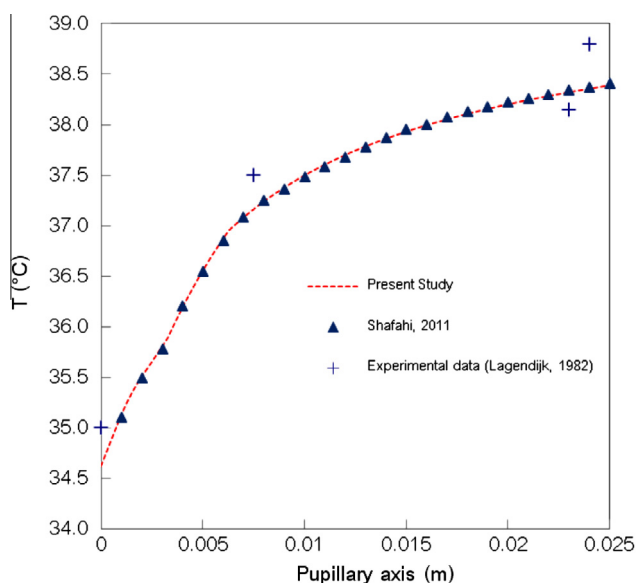

Fig. 6. Comparison of the calculated temperature distribution to the temperature distribution obtained by Shafahi and Vafai, and the Lagendijk's experimental data; h_{am} = 20 W/m² K and T_{am} = 25 °C.
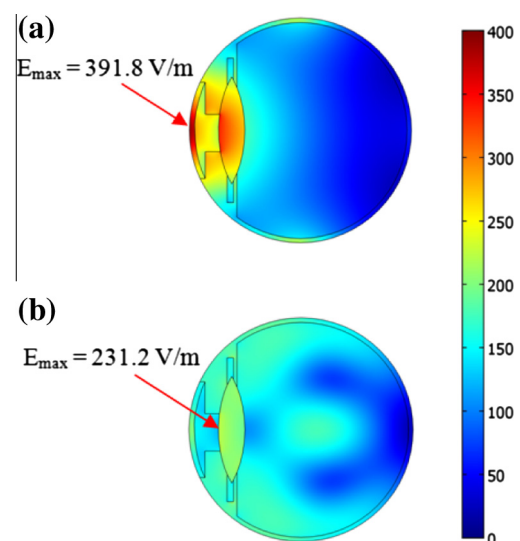

Fig. 7. Electric field distribution (V/m) in human eye exposed to the EM power density of 100 mW/cm² at the frequencies of (a) 900 MHz and (b) 1800 MHz.
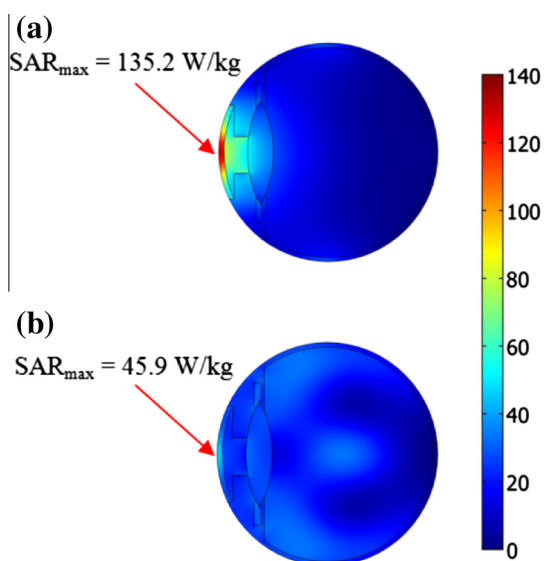
Fig. 8. SAR distribution (W/kg) in human eye exposed to the EM power density of 100 mW/cm² at the frequencies of (a) 900 MHz and (b) 1800 MHz.

4.3. SAR distribution

Fig. 8 shows the SAR distribution evaluated on the vertical cross section of the eye exposed to the EM frequencies of 900 and 1800 MHz. It is evident from the figure that the results of the SAR values in the eye (Fig. 8) are increased corresponding to the electric field intensities (Fig. 7). Besides the electric field intensity, the magnitude of the dielectric and thermal properties in each tissue will directly affect SAR values in the eye. For both frequencies, the highest SAR values are obtained in the region of the corneal surface. In this region, the frequencies of 900 and 1800 MHz display SAR values of 135.2 and 45.9 W/kg, respectively. This is because the cornea has a much higher value of its electrical conductivity (σ) than those of lens and iris. The second main reason is the position of the cornea located close to the exposed surface, at which the electric field intensity is strongest. It is found that the SAR distribution pattern in the eye, which corresponds to Eq. (5), is strongly depended on the effect of the dielectric properties (σ, shown in Table 1) and thermal properties (ρ, shown in Table 2). Moreover, the SAR pattern at the frequency of 1800 MHz shows a greater value of the EM power absorption in

the deep part of the eye, with less surface heating, compared to those of 900 MHz. Comparing to the ICNIRP standard for safety level at the maximum SAR value of 2 W/kg (general public exposure) and 10 W/kg (occupational exposure) [6], the resulting SAR values from this study are higher than the ICNIRP exposure limits for occupational exposure in all cases.

4.4. Temperature distribution

Since this study has focused on the volumetric heating effect into the multilayer tissues of the eye induced by EM fields, the effect of an ambient temperature variation have been neglected in order to gain insight into the interaction between the EM fields and the tissue as well as the correlation between the SAR and the heat transfer mechanism. For this reason, the ambient temperature has been set to the human body temperature of 37 °C, and the tear evaporation has been neglected. Moreover, the effect of thermoregulation mechanisms has also been neglected due to the small temperature increase occurred during exposure process. The convective coefficient due to the blood flow inside the sclera is set to 65 W/m² K [16]. In order to study the heat transfer in the eye, the coupled effects of EM wave propagation and unsteady heat transfer as well as the initial and boundary conditions are then investigated. Due to these coupled effects, the electric field distribution in Fig. 7 and the SAR distribution in Fig. 8 are then converted into heat by absorption of the tissue. Fig. 9 shows the temperature distribution in the vertical cross section human eye at various time exposed to the EM frequencies of 900 (Fig. 9(a)) and 1800 MHz (Fig. 9(b)). For the eye exposed to the EM fields for a period of time, the temperature in the eye (Fig. 9) is increased corresponding to the SAR (Fig. 8). This is because the electric fields in the eye attenuate owing to the energy absorbed and thereafter the absorbed energy is converted to thermal energy, which increases the eye temperature.

It is found that when the eye is subjected to the EM fields at different frequencies, the distribution patterns of temperature at a particular time are quite different. The hot spot zone is strongly displayed at the 10 min for two frequencies. Even the highest level of SAR values in both frequencies appears in the cornea (Fig. 8), the highest temperature for the frequency of 900 MHz is in the anterior chamber and for the frequency of 1800 MHz (Fig. 9) is the vitreous. This behavior is due to the fact that for the different frequency radiation at same radiated power, the temperature distribution pattern is not the same. In this case study, the difference in temperature distribution pattern between two chosen frequencies is caused by the dielectric properties of the tissue as well as
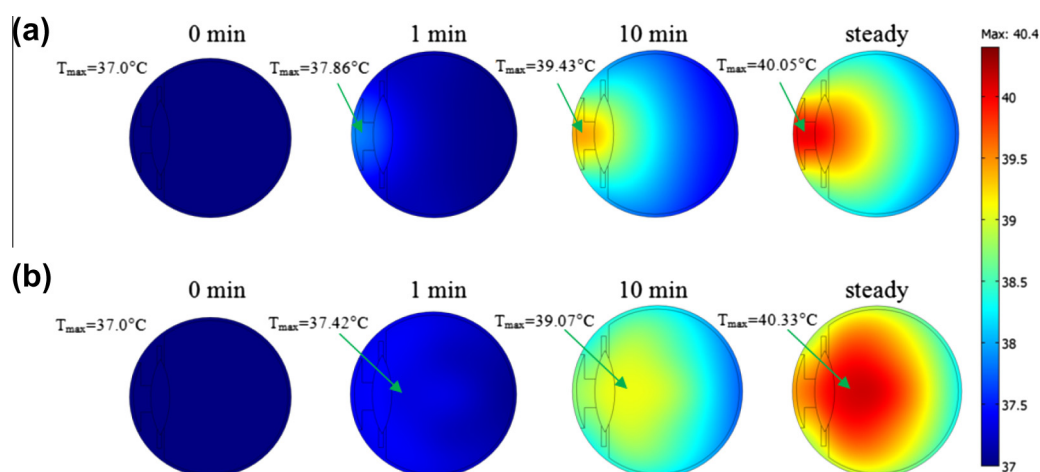

Fig. 9. The temperature distribution in human eye at various time exposed to the EM power density of 100 mW/cm² at the frequencies of (a) 900 MHz and (b) 1800 MHz.
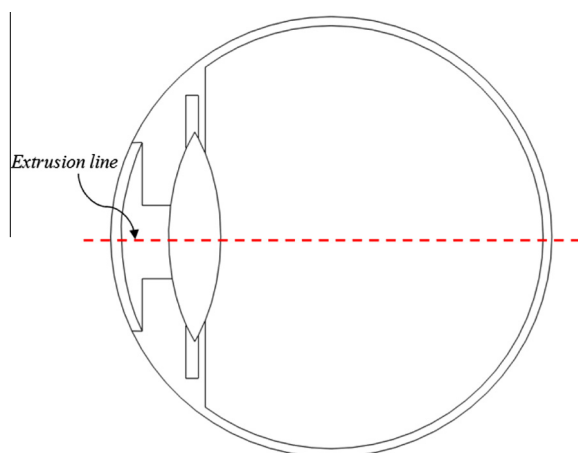
Fig. 10. The extrusion line in the eye where the temperature distribution is considered.

Fig. 11. Temperature increase versus papillary axis of human eye exposed to the EM frequencies of 900 and 1800 MHz at various times.

the electric field distribution pattern in the eye, which become the dominant mechanisms for the heat transfer.

For the 900 MHz frequency, even though the maximum values of the electric fields (Fig. 7(a)) and the SAR (Fig. 8(a)), are the cornea, the highest temperature is the anterior chamber (Fig. 9(a)). This is owing to the extensive penetration of the EM power of the internal regions and the higher dielectric properties (ε_r) of the anterior chamber. This higher dielectric property of the anterior chamber represents the stronger absorption ability of EM fields than those of cornea and lens. Moreover, the outer corneal surface has a lower temperature than that of the anterior chamber, even if it has higher SAR value (Fig. 8(a)). This is because, in this area, the generated heat is dissipated to the ambient via convection and radiation.

While for the 1800 MHz frequency, beside the cornea and lens, the high value of the electric fields is the middle of the vitreous and peripheral vitreous. This is owing to the constructive interference between the forward and reflected waves of the higher frequency of 1800 MHz results in standing wave patterns forming in the EM fields (Fig. 7(b)) in the vitreous area. This high electric field intensity increases the amount of energy absorption in the vitreous area (Fig. 8(b)) and consequently causes the temperature to rise (Fig. 9(b)). In this case, the maximum temperature increase in the peripheral vitreous area has a lower level than that of the middle of the vitreous even if the peripheral vitreous area also has high electric field intensity and the SAR value also. This is due to the presence of blood perfusion in the sclera tissue, which covers an internal surface area of the eye. This blood perfusion provides buffer characteristic to the eye temperature and plays important roles on the cooling processes in the peripheral vitreous area.

From the Fig. 9, it is found that the exposure time significantly influence the temperature increase in the eye. A longer exposure time resulted in a higher heat accumulation inside the eye, thereby increasing its temperature. By using the operating frequency of 900 MHz, the maximum temperatures increase are 0.86, 2.43, and 3.05 °C for the exposure times of 1 min, 10 min, and at steady-state conditions of 60 min, respectively. By using the operating frequency of 1800 MHz, the maximum temperatures increase are 0.42, 2.07, and 3.33 °C for the exposure times of 1 min, 10 min, and at steady-state conditions of 60 min, respectively.

Consider the temperature increase distribution at the extrusion line (Fig. 10). Fig. 11 shows the temperature increase versus papillary axis (along the extrusion line) of the eye exposed to the EM frequencies of 900 and 1800 MHz at various times. From the figure it is found that for every exposure time, the highest temperature for the frequency of 900 MHz is in the anterior chamber (in the
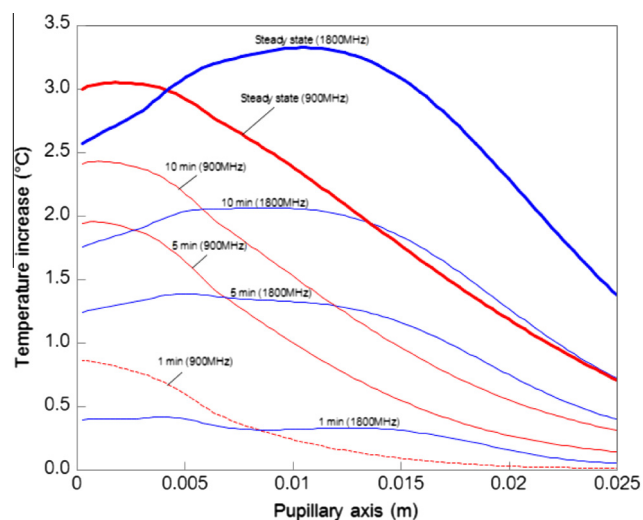
front part of the eye) and for the frequency of 1800 MHz is in the vitreous (in the middle part of the eye), as the reasons given previously. In the early stage of exposure (10 min), the temperature increase of the 900 MHz frequency is found to be higher than that of 1800 MHz frequency, especially in the front part of the eye. This is due to the high intensity of the electric fields and the SAR values in this area of the 900 MHz frequency, resulting in a high absorption of the EM energy.

In a steady state, the highest temperature for the frequency of 900 MHz is the anterior chamber, and for the frequency of 1800 MHz is still in the vitreous area. Surprisingly, in a steady state, the maximum temperature increase of the 1800 MHz frequency is higher than that of 900 MHz frequency. This is because not only does the anterior chamber have stronger absorption ability than that of other tissues but also the natural convection and radiation effects at the cornea surface play an important role in heat dissipation from the anterior chamber to the ambient. On the contrary, these heat dissipation effects in the vitreous area have worn off in perception rather than an enhancement. In the first period of exposure with the low flow speed of liquid in the anterior chamber (Fig. 12), the heat transfer in the anterior chamber occurs mainly by conduction across the fluid layer. While in a later time with higher flow speed induced by a higher temperature gradient, different flow regimes are encountered especially in the case of 900 MHz, with a progressively releasing heat into an environment and the connected tissue.

Fig. 12 shows the circulatory patterns in the anterior chamber in the eye exposed to the EM frequencies of 900 and 1800 MHz at various times. These patterns vary corresponding to the temperature gradient in the eye. Therefore, in the case of a lower temperature gradient, the circulatory patterns have a lower speed, where a circulatory pattern with a higher temperature gradient flows faster. For the 900 MHz frequency, it is found that the natural convection and formation of two circulatory patterns with opposite direction in the anterior chamber, shown in Fig. 12(a), play important roles on the cooling processes in the eye, especially in the inner corneal surface. It is observed that a large temperature gradient is significantly produced by the EM fields after 10 min. The circulation pattern implies that the generated heat in the anterior chamber is transferred in two directions; one is to the corneal surface, and the other to the lens surface. While for the 1800 MHz frequency, a counterclockwise circulation thus appears in the anterior chamber, shown in Fig. 12(b). This seemed to imply that the
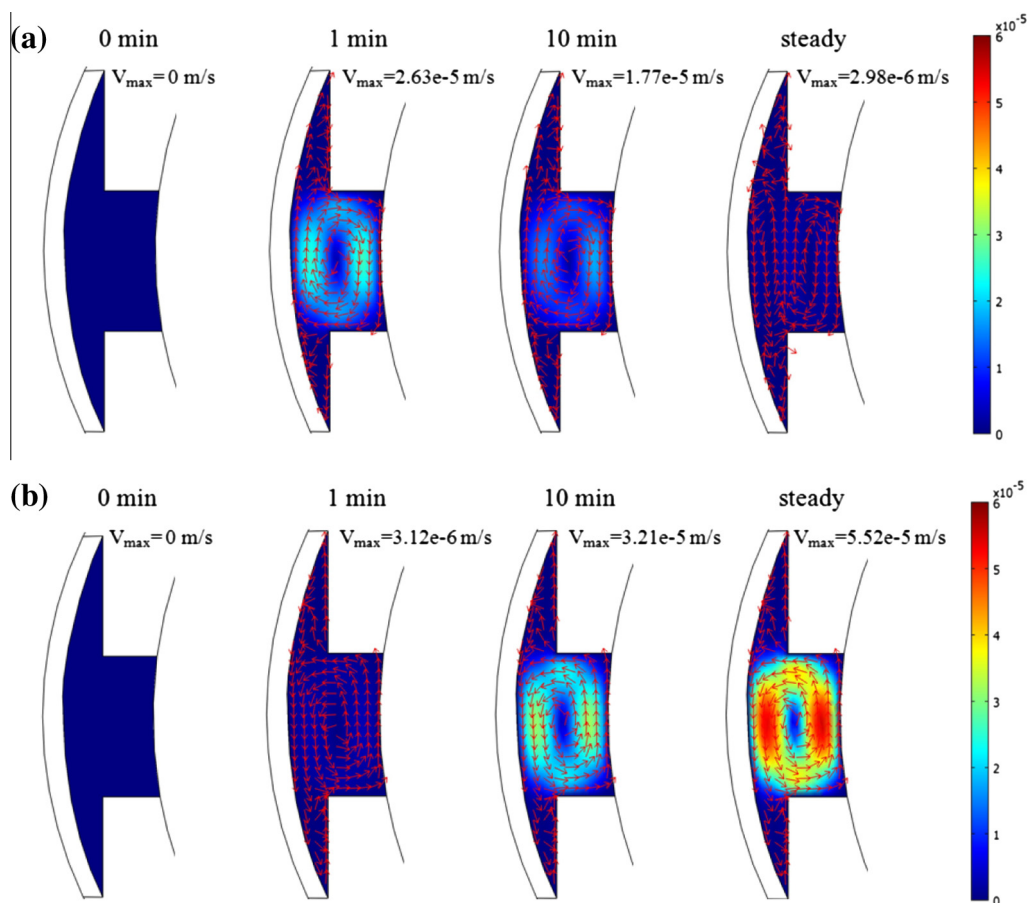
Fig. 12. The velocity distribution inside the anterior chamber at various time exposed to the EM power density of 100 mW/cm^2 at the frequencies of (a) 900 MHz and (b) 1800 MHz.

direction of heat transfer is travels outward from the lens surface. The circulation pattern in the 1800 MHz frequency is quite different from that of that of the 900 MHz frequency because of the different heating pattern in the eye between the two frequencies.

In this study, the maximum temperature increase in the eye exposed to the EM fields with the power density of 100 mW/cm^2 at the frequencies of 900 and 1800 MHz are 3.05 and 3.33 °C, respectively. The obtained temperature increases may leads to the formation of cataract or posterior capsular opacification [2].

5. Conclusions

The numerical simulations of the SAR and temperature distributions in this study show several important features of the energy absorption in the eye during exposed to the TM-mode of EM fields at 900 and 1800 MHz. In this study, the electric field distributions show a strong dependence on the dielectric properties of the tissue. The results of the SAR values are increased corresponding to the electric field intensities. Besides the electric field intensity, the magnitude of the dielectric and thermal properties in each tissue will directly affect the SAR values in the eye. It is found that the temperature distributions in the eye induced by the EM fields are not directly related to the SAR distribution due to the effect of the interaction among the dielectric properties, thermal properties, blood perfusion, and penetration depth of the EM power.

Therefore, health effect assessment of the EM field exposure requires the utilization of the most accurate numerical simulation of the thermal model along with the SAR model. In the future works, the effect of the ambient temperature variation will be included in the analysis to represent the actual heat transfer process which occurs in the realistic situation and will focus on the frequency-dependent dielectric properties of the tissue. A study will also be developed to a more realistic 3D model for simulations and to study the temperature dependency of dielectric property. This will allow a better understanding of the realistic situation of the interaction between the EM fields and the eye.

References

[1] A.F. Emery, P. Kramar, A.W. Guy, J.C. Lin, Microwave induced temperature rises in rabbit eyes in cataract research, ASME J. Heat Transfer 97 (1975) 123–128.
[2] C. Buccella, V.D. Santis, M. Feliaiani, Prediction of temperature increase in human eyes due to RF sources, IEEE Trans. Electromagn. Compat. 49 (4) (2007) 825–833.
[3] J.C. Lin, Cataracts and cell-phone radiation, IEEE Antennas Propag. Mag. 45 (1) (2003) 171–174.
[4] O. Fujiwara, A. Kato, Computation of SAR inside eyeball for 1.5-GHz microwave exposure using finite-difference time domain technique, IEICE Trans. E77-B (1994) 732–737.
[5] O.P. Gandhi, G. Lazzi, C.M. Furse, Electromagnetic absorption in the human head and neck for mobile telephones at 835 and 1900 MHz, IEEE Trans. Microwave Theor. Tech. 44 (10) (1996) 1884–1897.
[6] International Commission on Non-Ionizing Radiation Protection (ICNIRP), Guidelines for limiting exposure to time-varying electric, magnetic and electromagnetic fields (up to 300 GHz), Health Phys. 74, 1998, pp. 494–522.

[7] IEEE, IEEE standard for safety levels with respect to human exposure to radio frequency electromagnetic fields, 3 kHz to 300 GHz, IEEE standard C95.1, 1999.

[8] J.J.W. Lagendijk, A mathematical model to calculate temperature distribution in human and rabbit eye during hyperthermic treatment, Phys. Med. Biol. 27 (1982) 1301–1311.

[9] J. Scott, A finite element model of heat transport in the human eye, Phys. Med. Biol. 33 (1988) 227–241.

[10] J. Scott, The computation of temperature rises in the human eye induced by infrared radiation, Phys. Med. Biol. 33 (1988) 243–257.

[11] E.H. Amara, Numerical investigations on thermal effects of Laser–Ocular media interaction, Int. J. Heat Mass Transfer 38 (1995) 2479–2488.

[12] A. Hirata, S. Matsuyama, T. Shiozawa, Temperature rises in the human eye exposed to EM waves in the frequency range 0.6–6 GHz, IEEE Trans. Electromagn. Compat. 42 (4) (2000) 386–393.

[13] K.J. Chua, J.C. Ho, S.K. Chou, M.R. Islam, On the study of the temperature distribution within a human eye subjected to a laser source, Int. Commun. Heat Mass Transfer 32 (2005) 1057–1065.

[14] W. Limtrakarn, S. Reepolmaha, P. Dechaumphai, Transient temperature distribution on the corneal endothelium during ophthalmic phacoemulsification: a numerical simulation using the nodeless variable element, Asian Biomed. 4 (6) (2010) 885–892.

[15] S. Kumar, S. Acharya, R. Beuerman, A. Palkama, Numerical solution of ocular fluid dynamics in a rabbit eye: parametric effects, Ann. Biomed. Eng. 34 (2006) 530–544.

[16] E. Ooi, E.Y.K. Ng, Simulation of aqueous humor hydrodynamics in human eye heat transfer, Comput. Biol. Med. 38 (2008) 252–262.

[17] E.H. Ooi, E.Y.K. Ng, Effects of natural convection inside the anterior chamber, Int. J. Numer. Methods Biomed. Eng. 27 (2011) 408–423.

[18] H.H. Pennes, Analysis of tissue and arterial blood temperatures in the resting human forearm, J. Appl. Physiol. 1 (1948) 93–122.

[19] H.H. Pennes, Analysis of tissue and arterial blood temperatures in the resting human forearm, J. Appl. Physiol. 85 (1) (1998) 5–34.

[20] V.M.M. Flyckt, B.W. Raaymakers, J.J.W. Lagendijk, Modeling the impact of blood flow on the temperature distribution in the human eye and the orbit: fixed heat transfer coefficients versus the pennes bioheat model versus discrete blood vessels, Phys. Med. Biol. 51 (2006) 5007–5021.

[21] E.Y.K. Ng, E.H. Ooi, FEM simulation of the eye structure with bioheat analysis, Comput. Methods Programs Biomed. 82 (2006) 268–276.

[22] E.H. Ooi, E.Y.K. Ng, Ocular temperature distribution: a mathematical perspective, J. Mech. Med. Biol. 9 (2009) 199–227.

[23] A. Nakayama, F. Kuwahara, A general bioheat transfer model based on the theory of porous media, Int. J. Heat Mass Transfer 51 (2008) 3190–3199.

[24] S. Mahjoob, K. Vafai, Analytical characterization of heat transfer through biological media incorporating hyperthermia treatment, Int. J. Heat Mass Transfer 52 (2009) 1608–1618.

[25] K. Khanafer, K. Vafai, Synthesis of mathematical models representing bioheat transport, Adv. Numer. Heat Transfer 3 (2009) 1–28.

[26] M. Shafahi, K. Vafai, Human eye response to thermal disturbances, ASME J. Heat Transfer 133 (2011) 011009.

[27] E.H. Ooi, W.T. Ang, E.Y.K. Ng, A boundary element model of the human eye undergoing laser thermokeratoplasty, Comput. Biol. Med. 28 (2008) 727–738.

[28] E.H. Ooi, W.T. Ang, E.Y.K. Ng, A boundary element model for investigating the effects of eye tumor on the temperature distribution inside the human eye, Comput. Biol. Med. 28 (2009) 727–738.

[29] J.H. Tan, E.Y.K. Ng, U.R. Acharya, C. Chee, Study of normal ocular thermogram using textural parameters, Infrared Phys. Technol. 53 (2010) 120–126.

[30] J.H. Tan, E.Y.K. Ng, U.R. Acharya, Evaluation of tear evaporation from ocular surface by functional infrared thermography, Med. Phys. 37 (2010) 6022–6034.

[31] J.H. Tan, E.Y.K. Ng, U.R. Acharya, Evaluation of topographical variation in ocular surface temperature by functional infrared thermography, Infrared Phys. Technol. 54 (2011) 469–477.

[32] T. Wessapan, S. Srisawatdhisukul, P. Rattanadecho, Numerical analysis of specific absorption rate and heat transfer in the human body exposed to leakage electromagnetic field at 915 MHz and 2450 MHz, ASME J. Heat Transfer 133 (2011) 051101.

[33] T. Wessapan, S. Srisawatdhisukul, P. Rattanadecho, The effects of dielectric shield on specific absorption rate and heat transfer in the human body exposed to leakage microwave energy, Int. Commun. Heat Mass Transfer 38 (2011) 255–262.

[34] T. Wessapan, P. Rattanadecho, Numerical analysis of specific absorption rate and heat transfer in human head subjected to mobile phone radiation, ASME J. Heat Transfer 134 (2012) 121101.

[35] T. Wessapan, S. Srisawatdhisukul, P. Rattanadecho, Specific absorption rate and temperature distributions in human head subjected to mobile phone radiation at different frequencies, Int. J. Heat Mass Transfer 55 (2012) 347–359.

[36] P. Keangin, T. Wessapan, P. Rattanadecho, Analysis of heat transfer in deformed liver cancer modeling treated using a microwave coaxial antenna, Appl. Therm. Eng. 31 (16) (2011) 3243–3254.

[37] P. Keangin, T. Wessapan, P. Rattanadecho, An analysis of heat transfer in liver tissue during microwave ablation using single and double slot antenna, Int. Commun. Heat Mass Transfer 38 (2011) 757–766.

[38] T. Wessapan, P. Rattanadecho, Specific absorption rate and temperature increase in human eye subjected to electromagnetic fields at 900 MHz, ASME J. Heat Transfer 134 (2012) 091101.

[39] P. Bernardi, M. Cavagnaro, S. Pisa, E. Piuzzi, Specific absorption rate and temperature increases in the head of a cellular-phone user, IEEE Trans. Microwave Theor. Tech. 48 (7) (2000) 1118–1126.

[40] S. Park, J. Jeong, Y. Lim, Temperature rise in the human head and brain for portable handsets at 900 and 1800 MHz, in: Proceedings of the Fourth International Conference on Microwave and Millimeter Wave Technology, vol. 1, 2004, pp. 966–969.